

# Preparation and properties of $\beta$ -CaSiO<sub>3</sub>/ZrO<sub>2</sub> (3Y) nanocomposites

Lihua Long<sup>a,c</sup>, Faming Zhang<sup>b</sup>, Lei Chen<sup>b</sup>, Lidong Chen<sup>a</sup>, Jiang Chang<sup>b,\*</sup>

<sup>a</sup> State Key Laboratory of High Performance Ceramics & Superfine Microstructure, Shanghai Institute of Ceramics, Chinese Academy of Sciences, Shanghai 200050, China

<sup>b</sup> Biomaterials and Tissue Engineering Research Center, Shanghai Institute of Ceramics, Chinese Academy of Sciences, Shanghai 200050, China

<sup>c</sup> Graduate School of Chinese Academy of Science, Shanghai 200050, China

Received 17 March 2008; received in revised form 7 May 2008; accepted 14 May 2008

Available online 25 June 2008

## Abstract

$\beta$ -CaSiO<sub>3</sub>/ZrO<sub>2</sub> (3Y) nanocomposites were successfully fabricated by spark plasma sintering (SPS) technique. The addition of nanocrystalline ZrO<sub>2</sub> could inhibit the phase transition of micrometer sized CaSiO<sub>3</sub> and increase its phase transitional temperature. The relative densities of the dense  $\beta$ -CaSiO<sub>3</sub>/ZrO<sub>2</sub> nanocomposites were above 98%. Nanocrystalline ZrO<sub>2</sub> has formed a network structure in the nanocomposites, which could improve the mechanical properties of nanocomposites. The fracture strength and fracture toughness of the nanocomposites were as high as 395 MPa and 4.08 MPa m<sup>1/2</sup>, respectively. The nanocomposites showed good *in vitro* bioactivity with hydroxyapatite (HA) layer formation on the ZrO<sub>2</sub> network of the nanocomposites in simulated body fluid. The spark plasma sintered  $\beta$ -CaSiO<sub>3</sub>/ZrO<sub>2</sub> (3Y) nanocomposite may provide a new bone graft for load bearing applications.

© 2008 Elsevier Ltd. All rights reserved.

**Keywords:** Nanocomposites; Mechanical properties; ZrO<sub>2</sub>

## 1. Introduction

Wollastonite (CaSiO<sub>3</sub>, CS) is a novel biomaterial and has excellent bioactivity.<sup>1</sup> Many researches were focused on its application as a promising bone repair material.<sup>1–4</sup> However, the wollastonite bioceramics are difficult to be densified by conventional sintering methods, by which the relative density is below 90%, bending strength below 100 MPa, and fracture toughness ( $K_{IC}$ ) below 1 MPa m<sup>1/2</sup>.<sup>5</sup> In our previous study,  $\beta$ -CaSiO<sub>3</sub> bioceramics with relative density of 95% were fabricated at 950 °C by spark plasma sintering (SPS).<sup>6</sup> These dense wollastonite bioceramics exhibited excellent bending strength about 294 MPa, and suitable Young's modulus about 46 GPa.<sup>6</sup> However, their fracture toughness (1.54 MPa m<sup>1/2</sup>) was still low and not satisfactory for load bearing applications as bone repair material.

Zirconia (ZrO<sub>2</sub>) ceramic with high toughness has been applied in the biomedical field due to its reliable mechanical performance and bioinert biological properties.<sup>7,8</sup> In some cases,

ZrO<sub>2</sub> was used to reinforce some brittle bioceramics such as hydroxyapatite (HA) to improve their mechanical properties especially fracture toughness.<sup>9,10</sup> In this study, nanocrystalline ZrO<sub>2</sub> (3Y) was incorporated into the micrometer sized  $\beta$ -CaSiO<sub>3</sub> matrix to increase its mechanical properties, and the  $\beta$ -CaSiO<sub>3</sub>/ZrO<sub>2</sub> nanocomposites were fabricated by SPS technique. The sintering behavior, microstructures, mechanical properties, and *in vitro* bioactivity were investigated.

## 2. Materials and methods

Wollastonite ( $\beta$ -CaSiO<sub>3</sub>) and ZrO<sub>2</sub> (3Y) powders were used in the study. The synthetic method and particle morphology of the  $\beta$ -CaSiO<sub>3</sub> powder were investigated in our previous work.<sup>6</sup> The commercial nano-sized ZrO<sub>2</sub> (3Y) powder was obtained from Toso Co., Tokyo, Japan. The two kinds of powders were mixed with different  $\beta$ -CaSiO<sub>3</sub>/ZrO<sub>2</sub> mole ratio of 80/20 (abbreviated as C8Z2), 60/40 (C6Z4) and 40/60 (C4Z6) by ball milling. The obtained powder mixtures were put into a graphite die with 30 mm in diameter, and then subjected for spark plasma sintering (Dr. Sinter 2040, Sumitomo Coal Mining Co.) in vacuum (<10<sup>-4</sup> Pa) under a pressure of 40 MPa.

\* Corresponding author. Tel.: +86 21 52412804; fax: +86 21 52413903.  
E-mail address: [jchang@mail.sic.ac.cn](mailto:jchang@mail.sic.ac.cn) (J. Chang).

Table 1

The relative density and phases of the spark plasma sintered samples with various ZrO<sub>2</sub> contents at different temperatures

Content of ZrO <sub>2</sub>		Sintering temperature (°C)	Phase	Relative density (%)
mol%	vol.%			
0	0	950	β-CS	95
		970	α-CS	99
20	10	950	β-CS + TZP	90
		970	β-CS + TZP	93
		1000	α-CS + TZP	98
40	20	1000	β-CS + TZP	95
		1020	β-CS + TZP	99
		1050	α-CS + TZP	98
60	45	1020	β-CS + TZP	93
		1050	β-CS + α-CS + TZP	98
		1080	α-CS + TZP	98

The heating rate was 150–200 °C/min and the holding time was 5 min.

The phases of the powder and sintered specimens were analyzed by XRD (Rigaku D/max 2200PC). The density was determined by Archimedes method. Microstructures analysis was performed by scanning electron microscopy (JOEL, JSM-6700F). The bending strength and Young's modulus were measured using a three-point method with a span length of 20 mm by a Instron-1195 tester at crosshead speed of 0.5 mm/min. Indentation tests were employed to determine the fracture toughness using a Vickers' diamond indenter (Instron-2100B) with 5 Kg loads and 10 s dwell time. Six samples of each group were measured for statistical analysis. The C6Z4 nanocomposites were selected and soaked in simulated body fluid (SBF) to evaluate the *in vitro* bioactivity of sintered composites. The SBF was prepared according to the procedure described by Kokubo et al.<sup>11</sup> The soaking time was 3, 7, 14 and 21 days and the SBF was renewed everyday. The soaking temperature was maintained at 36.5 °C.

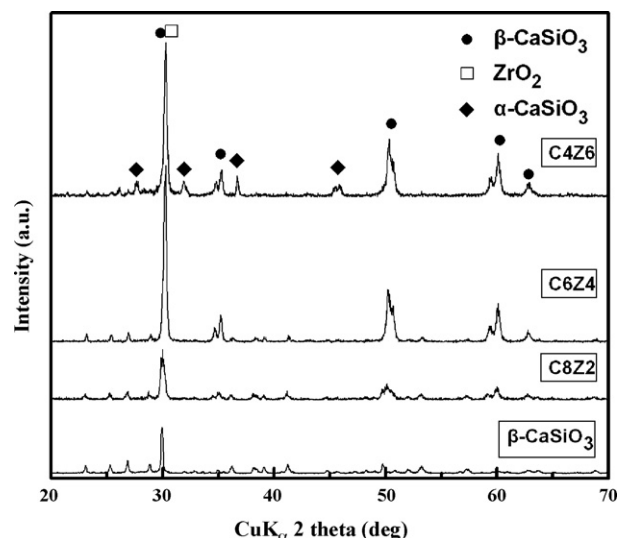
### 3. Results and discussion

Several samples with different zirconia contents were prepared at various temperatures by SPS. Table 1 showed that the CaSiO<sub>3</sub> bioceramics kept their low temperature β phase, and showed relative density of about 95%. After sintering at 970 °C, the β-CaSiO<sub>3</sub> has transformed into α-CaSiO<sub>3</sub>. The density of α-CaSiO<sub>3</sub> reached about 99%; however, their mechanical properties were very low. Therefore, the formation of α-CaSiO<sub>3</sub> should be avoided. When the content of ZrO<sub>2</sub> was increased to 20 mol%, the β-CaSiO<sub>3</sub> was maintained after sintering at 970 °C. The phase transitional temperature of the β-CaSiO<sub>3</sub> was at 1000 °C. There were few α-CaSiO<sub>3</sub> phases in the composites that sintered at 1050 °C for the C6Z4 samples, and the β-CaSiO<sub>3</sub> transformed into their α phase completely at 1080 °C. The phase transitional temperature increased with the increase of the ZrO<sub>2</sub> content.

The high-density samples with different contents of ZrO<sub>2</sub> were selected for further investigation. They were β-CS, C8Z2 (970 °C), C6Z4 (1020 °C) and C4Z6 (1050 °C) composites. The

XRD results for the above nanocomposites are shown in Fig. 1. As shown in Fig. 1, wollastonite still kept β-CaSiO<sub>3</sub> phase (low temperature phase) after sintered at 950 °C by SPS. The main peaks of β-CaSiO<sub>3</sub> ( $2\theta = 29^\circ$ ) and ZrO<sub>2</sub> ( $2\theta = 30^\circ$ ) were so close that their content was difficult to be measured. However, the strong peaks of β-CaSiO<sub>3</sub> at  $2\theta = 23.1, 25.4, 26.9$  and  $29^\circ$  decreased and the peaks of ZrO<sub>2</sub> increased at  $2\theta = 30, 35, 50$  and  $60^\circ$  with the increase in ZrO<sub>2</sub> content. The strongest peaks of β-CaSiO<sub>3</sub> and ZrO<sub>2</sub> matched together and formed the strongest peak of the composites.

Fig. 2 shows the SEM micrographs of the β-CS/ZrO<sub>2</sub> nanocomposites. In the backscattered SEM images, the bright field was ZrO<sub>2</sub> phase and the dark one was β-CaSiO<sub>3</sub> phase (Fig. 2a and b). The β-CaSiO<sub>3</sub> phase with size of 1 μm was encapsulated by ZrO<sub>2</sub> phase. The ZrO<sub>2</sub> formed a continuous network in the C6Z4 composites with corresponding volume content of about 20%. The continuous network contributes to the increase of the mechanical properties of the nanocomposites. In C4Z6 samples, the content of the ZrO<sub>2</sub> phase was higher. The β-CaSiO<sub>3</sub> phase was enclosed by ZrO<sub>2</sub> phase nonuniformly. The

Fig. 1. XRD patterns of β-CS ceramics and β-CS/ZrO<sub>2</sub> nanocomposites.

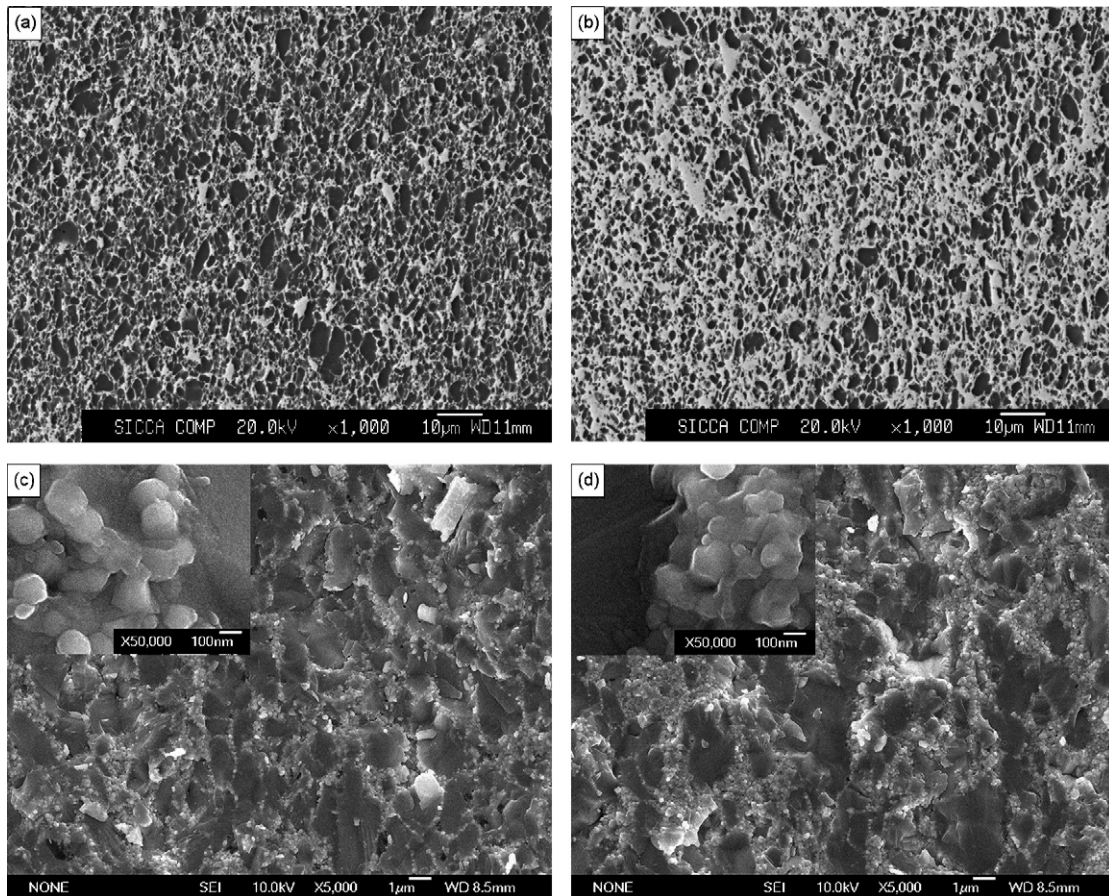


Fig. 2. The SEM backscattered (a and b) and secondary electron images (c and d) of the C6Z4 (a and c) and C4Z6 (b and d) nanocomposites.

secondary SEM images of the cross-section of the nanocomposites were shown in Fig. 2c and d. The C6Z4 and C4Z6 samples were fully densified without any micropores. The ZrO<sub>2</sub> grains showed marginal grain growth. It found in the insert images that the grain size of ZrO<sub>2</sub> was about 100 nm. The ZrO<sub>2</sub> grains unevenly distributed throughout the nanocomposites.

Table 2 shows the mechanical properties of the prepared nanocomposites by SPS. It is clear to see that the fracture strength of the pure  $\beta$ -CaSiO<sub>3</sub> ceramics was about 294 Mpa, while the fracture strength of the C8Z2 samples was 255 Mpa. Comparison of the relative density of both ceramics (see Table 1), a lower relative density of C8Z2 (93%) was evident as compared with that of pure  $\beta$ -CaSiO<sub>3</sub> ceramics (95%). Previous studies have shown that the mechanical strengths of the sintered ceramics were correlated with the densification.<sup>12,13</sup> It is assumed that the relative density is the key factor to affect the fracture strength of the two ceramics. However, when the ZrO<sub>2</sub> content further increased to 40 and 60 mol%, the fracture strength increased up to 518 MPa, even when the relative density of the C6Z4 and C4Z6 maintained at low level of 93–95%. In this situation, the ZrO<sub>2</sub> content becomes the dominant factor to determine the fracture strength of the composite ceramics. In the case of the fracture toughness, it is observed that the fracture toughness increased with the increase of the ZrO<sub>2</sub> content, reached a maximum of 4.08 MPa m<sup>1/2</sup> at the 40 mol% ZrO<sub>2</sub>, and then decreased to 3.10 MPa m<sup>1/2</sup> with further increase of the

ZrO<sub>2</sub> content, which might be related to the phase transformation of  $\beta$ -CaSiO<sub>3</sub> in the C6Z4 samples. The Young's modulus of the nanocomposites was increased with the increase of the ZrO<sub>2</sub> content accordingly.

In our previous work, the  $\beta$ -CaSiO<sub>3</sub> transformed into  $\alpha$ -CaSiO<sub>3</sub> on 970 °C during SPS processing resulted in a great

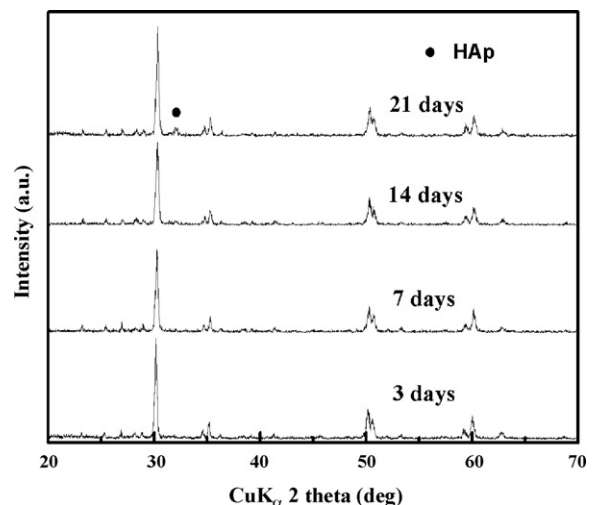


Fig. 3. XRD patterns of the C6Z4 nanocomposites soaked in SBF for various periods.

Table 2  
The mechanical properties of the  $\beta$ -CS/ZrO<sub>2</sub> nanocomposites

Content of zirconia (mol%)	Fracture strength $\sigma_f$ (MPa)	Fracture toughness $K_{IC}$ MPa m <sup>1/2</sup>	Young's modulus (GPa)
0	294 ± 11	1.54 ± 0.04	46.5 ± 5.0
20	255 ± 6	2.21 ± 0.08	52.5 ± 4.0
40	395 ± 7	4.08 ± 0.13	81.0 ± 4.2
60	518 ± 18	3.10 ± 0.07	96.0 ± 7.1

decrease of mechanical properties.<sup>6</sup> In this study, the sintering temperature of the nanocomposites was increased with the content of ZrO<sub>2</sub>. And there were few  $\beta$ -CaSiO<sub>3</sub> transformed into  $\alpha$ -CaSiO<sub>3</sub> at 1050 °C in C4Z6 samples. The relative densities

of the C6Z4 and C4Z6 were above 99%. On the other hand, the ZrO<sub>2</sub> phase showed a network structure in the matrix. Therefore, the mechanical properties, especially fracture strength and fracture toughness, were improved greatly. In our study, the fracture

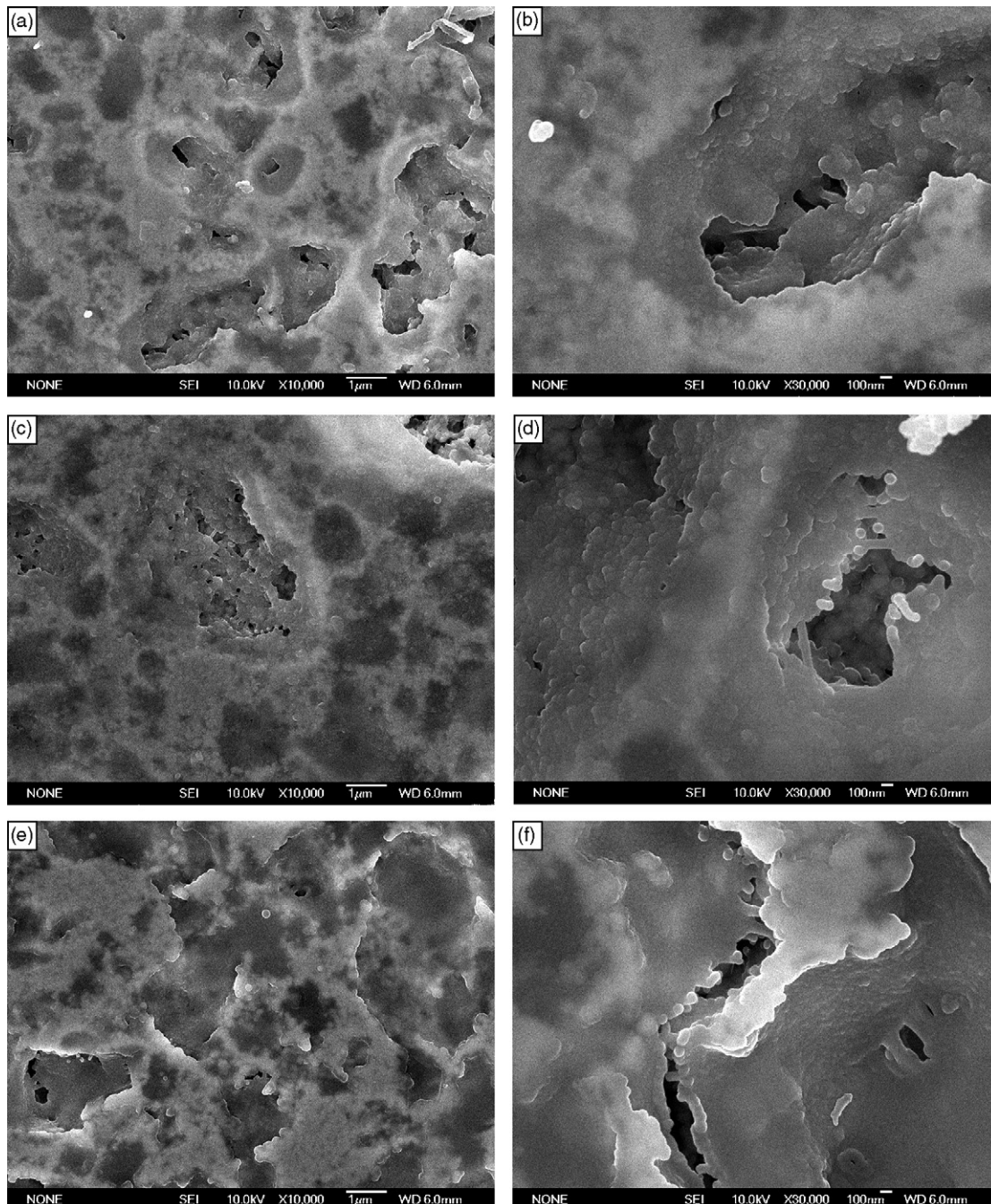


Fig. 4. SEM micrographs of the surfaces of the C6Z4 nanocomposites after soaking in SBF for 7 (a and b), 14 (c and d) and 21 (e and f) days.

strength and fracture toughness of the C6Z4 samples increased about 100 MPa and  $2.5 \text{ MPa m}^{1/2}$  by mixed 40 mol%  $\text{ZrO}_2$  when compared with the pure  $\beta\text{-CaSiO}_3$  bioceramics.

The C6Z4 composites were polished and immersed in SBF to evaluate their *in vitro* bioactivity. Fig. 3 shows the XRD patterns of C6Z4 composites soaked for different periods. The main peaks of hydroxyapatite could not be observed after soaking for 3 and 7 days in SBF. The main peak of HA ( $2\theta = 32^\circ$ ) was detected after soaking for 14 and 21 days. The results showed that there HA formed on the surface of C6Z4 after soaking in the SBF. Fig. 4 shows the surface micrographs of the composites after soaking in the SBF for 7, 14 and 21 days. There were many pits on the surface of the sample immersed in the SBF for 7 days, which might be due to dissolution of  $\text{CaSiO}_3$ . The pits became shallow and silkworm-like HA particles were formed after 14 days soaking. After soaking for 21 days, the HA deposited on the surface continuously and the pits were also filled by HA. There were some HA cracks on the surface, it was due to the HA dehydration during drying. The incorporation of nanocrystalline  $\text{ZrO}_2$  into the micrometer sized  $\beta\text{-CaSiO}_3$  matrix has improved its mechanical properties, and at the same time kept its *in vitro* bioactivity. The surface of the nanocomposites soaked in SBF was similar to porous biomaterials (Fig. 4a and b). It may be helpful to improve the integration between bone tissue and the nanocomposites after being implanted *in vivo*. The nanocomposites exhibited excellent mechanical properties and may be suitable for load bearing bone grafts. In general, the spark plasma sintered  $\beta\text{-CaSiO}_3/\text{ZrO}_2$  (3Y) nanocomposite may provide a new bone graft for load bearing applications.

#### 4. Conclusions

$\beta\text{-CaSiO}_3/\text{ZrO}_2$  (3Y) nanocomposites were successfully fabricated by spark plasma sintering technique. The addition of  $\text{ZrO}_2$  could inhibit the phase transition of  $\text{CaSiO}_3$  and increase its phase transitional temperature. The relative densities of the dense  $\beta\text{-CaSiO}_3/\text{ZrO}_2$  nanocomposites were above 98%. A nanocrystalline  $\text{ZrO}_2$  network structure was formed in the nanocomposites, and this network improved the mechanical properties of nanocomposites. The fracture strength and fracture toughness of the C6Z4 nanocomposites were 395 MPa and  $4.08 \text{ MPa m}^{1/2}$ , respectively. The C6Z4 composites showed good *in vitro* bioactivity with HA layer formation on the  $\text{ZrO}_2$  network of the nanocomposites in SBF. The spark plasma sintered

$\beta\text{-CaSiO}_3/\text{ZrO}_2$  (3Y) nanocomposite may provide a new bone graft for load bearing applications.

#### Acknowledgements

This work is supported by the National Basic Science Research Program of China (973 Program) (Grant No.: 2005CB522704), the Funds of the Chinese Academy of Sciences for Key Topics in Innovation Engineering (Grant No.: KGCX2-YW-207) and the Funds of the Shanghai Institute of Ceramics Chinese Academy of Sciences for Innovation of Science and Technology (Grant No.: SCX0606).

#### References

- De Aza, P. N., Guitian, F. and De Aza, S., Bioactivity of wollastonite ceramics: in vitro evaluation. *Scripta Metallurgica et Materialia*, 1994, **31**, 1001–1005.
- Siyu, Ni, Jiang, Chang and Lee, Chou, A novel bioactive porous  $\text{CaSiO}_3$  scaffold for bone tissue engineering. *J. Biomed. Mater. Res. A*, 2006, **76**, 196–205.
- Hazar, A. and Binnaz Yoruc, Preparation and in vitro bioactivity of  $\text{CaSiO}_3$  powders. *Ceram. Int.*, 2007, **33**, 687–692.
- Li, Lin Kai, Jiang, Chang and Zheng, Wang, Fabrication and the characterisation of the bioactivity and degradability of macroporous calcium silicate bioceramics in vitro. *J. Inorg. Mater.*, 2005, **20**(3), 692–698.
- Lin, K. L., Zhai, W. Y., Ni, S. Y., Chang, J., Zeng, Y. and Qian, W., Study of the mechanical property and in vitro biocompatibility of  $\text{CaSiO}_3$  ceramics. *Ceram. Int.*, 2005, **31**, 323–326.
- Long, L. H., Chen, L. D., Bai, S. Q., Chang, J. and Lin, K. L., Preparation of dense- $\text{CaSiO}_3$  ceramic with high mechanical strength and HAp formation ability in simulated body fluid. *J. Eur. Cer. Soc.*, 2006, **26**, 1701–1706.
- Piconi, C. and Maccauro, G., Zirconia as a ceramic biomaterial. *Biomaterials*, 1999, **20**, 1–25.
- Chevalier, Jerome, What future for zirconia as a biomaterial? *Biomaterials*, 2006, **27**, 535–543.
- Silva, Viviane V., Lameiras, Fernando S. and Domingues, Rosana Z., Microstructural and mechanical study of zirconia-hydroxyapatite (ZH) composite ceramics for biomedical applications. *Compos. Sci. Technol.*, 2001, **61**, 301–310.
- Kutty, Muralithran G., Bhaduri, S. and Bhaduri, S. B., The effects of zirconia additions on the sintering behaviour and phase stability of hydroxyapatite ceramics. *Ceramic Eng. Sci. Proc.*, 2001, **22**, 601–606.
- Tadashi, Kokubo and Hiroaki, Takadama, How useful is SBF in predicting in vivo bone bioactivity? *Biomaterials*, 2006, **27**, 2907–2915.
- Shi, J. L., Thermodynamics and densification kinetics in solidstate sintering of ceramics. *J. Mater. Res.*, 1999, **14**, 1398–1408.
- Rice, R. W., Grain size and porosity dependence of ceramic fracture energy and toughness at  $22^\circ\text{C}$ . *J. Mater. Sci.*, 1996, **31**, 1969–1983.